Validation Testing of the Prediction Accuracy of the Numerical Wind Synopsis Prediction Technique RIAM-COMPACT【○!R】 for the Case of the Bolund Experiment

Uchida, Takanori
Research Institute for Applied Mechanics, Kyushu University

https://doi.org/10.15017/1526213

出版情報：九州大学応用力学研究所所報. 147, pp.7-14, 2014-09. Research Institute for Applied Mechanics, Kyushu University
バージョン：
権利関係：

Validation Testing of the Prediction Accuracy of the Numerical Wind Synopsis Prediction Technique RIAM-COMPACT® for the Case of the Bolund Experiment

- Comparison against a Wind-Tunnel Experiment -

Takanori UCHIDA*1

E-mail of corresponding author: *takanori@riam.kyushu-u.ac.jp*

(Received July 31, 2014)

Abstract

In the present study, wind conditions were numerically predicted for the site of the Bolund Experiment using the RIAM-COMPACT® natural terrain version software, which is based on an LES turbulence model (CFD). In addition, airflow measurements were made using a split-fiber probe in the boundary layer wind tunnel of the Institute of Industrial Science, University of Tokyo (a facility of the research group of Prof. Chisachi Kato). The characteristics of the airflow at and in the vicinity of the site of the Bolund Experiment were clarified. The study also examined the prediction accuracy of the LES turbulence simulations (CFD). The values of the streamwise (x) wind velocity predicted by the CFD model were generally in good agreement with those from the wind tunnel experiment at all points and heights examined, demonstrating the validity of CFD based on LES turbulence modeling.

Key words : Bolund Experiment, Wind tunnel experiment, RIAM-COMPACT®

1. Introduction

Recently, the wind power industry has undergone rapid growth at an unprecedented rate across the world. This growth has been occurring because wind power generation has the best cost performance of all the renewable energies in terms of achieving a post-fossil fuel society and reducing CO_2 emissions. There is no doubt that wind power is the leading renewable energy even in Japan. The authors are convinced that further dissemination of wind power generation will contribute on the global scale to "green innovation", efforts to combat global warming.

In the field of wind power generation, as is the case in other fields, the use of CFD (Computational Fluid Dynamics) has increased rapidly and is being used for wind turbine deployment planning and estimation of the annual energy production of wind turbines. Given this background, validation testing of the prediction accuracy of CFD software used in the field of wind power generation has been advanced by various interested groups. One such validation testing was conducted as part of the Bolund Experiment (see Fig. 1). In this project, which was led by Risø DTU (Technical University of Denmark), the flow field passing over an isolated topographical feature protruding above the sea surface was targeted. During this project, wind condition observations (by cup and ultrasonic anemometers and LIDAR) and numerical simulations (CFD simulations) were performed; furthermore, based on these results, the prediction accuracy of CFD simulations has been analyzed. In these analyses, RANS (Reynolds Averaged Navier-Stokes) models (time-averaged models), which are steady, nonlinear wind analysis models, have received more favorable evaluations than LES (Large-Eddy Simulation) models (spatial-averaged models), which are unsteady, nonlinear wind analysis models. In contrast, in Japan, LES models as well as RANS models have received favorable evaluations. Accordingly, the present study re-examines the accuracy of airflow predictions by an LES model. For this purpose, the author conducted an independent wind tunnel experiment for the airflow over the topography studied in the Bolund Experiment. The present study compares the results from the LES-based numerical

Fig. 1 The topography studied in the Bolund

*1 Research Institute for Applied Mechanics, Kyushu University

wind synopsis prediction technique RIAM-COMPACT®, which was developed and is continuing to be developed by the author's research group, and the airflow measurement results from the wind tunnel experiment.

2. Overview of the RIAM-COMPACT® Natural Terrain Version Software

The core technology of RIAM-COMPACT® (Research Institute for Applied Mechanics, Kyushu University, COMputational Prediction of Airflow over Complex Terrain) is under continuous development at the Research Institute for Applied Mechanics, Kyushu University[1]. An exclusive license of the core technology has been granted by Kyushu TLO Co., Ltd. (Kyushu University TLO) to RIAM-COMPACT Co., Ltd. (http://www.riam-compact.com/), a venture corporation which was founded by the author and others and originated at Kyushu University in 2006. (A trademark, RIAM-COMPACT®, and a utility model patent were granted to RIAM-COMPACT Co., Ltd. in the same year.) In the meantime, a software package has been developed based on the above-mentioned technique and is named the RIAM-COMPACT® natural terrain version software. A development consortium has also been formed for this software, consisting of RIAM-COMPACT Co., Ltd., West Japan Engineering Consultants, Inc. (a member of the Kyushu Electric Group), and Environmental GIS Laboratory Co., Ltd. The consortium has been working together to promote the software as a standard model throughout the industry. As of today, the RIAM-COMPACT® software has been used by a large number of corporations and institutions including Electric Power Development Co., Ltd. (J-POWER), Japan Wind Development Co., Ltd., Eco Power Co., Ltd., and Eurus Energy Japan Corporation, which has the largest share of the wind power generation industry in Japan.

Computation time had been an issue of concern for the RIAM-COMPACT® software, which focuses on unsteady turbulence simulations. However, the present fluid simulation solver is compatible with multi-core CPUs (Central Processing Units) such as the Intel Core i7, which has drastically reduced the computation time, leaving no appreciable problems in terms of the practical use of the RIAM-COMPACT® software.

Furthermore, the RIAM-COMPACT® software has successfully been made compatible with GPGPU (General Purpose computing on Graphics Processing Units). The concept of GPGPU is to widely apply the floating-point operation capacity of a GPU not only to graphics rendering but also to other numerical operations.

Subsequently, the numerical technique used for RIAM-COMPACT® is described. Collocated grids in a general curvilinear coordinate system are used for the arrangement of variables in order to numerically predict local airflows over complex terrain with high accuracy while avoiding numerical instability. In these collocated grids, the velocity components and pressure are defined at the grid cell centers, and variables which result from the contravariant velocity components multiplied by the Jacobian are defined at the cell faces. As for the numerical method, the FDM (Finite-Difference Method) is adopted, and an LES model is used for the turbulence model. In LES, a spatial filter is applied to the flow field to separate eddies of various scales into GS (Grid Scale) components, which are larger than the computational grid cells, and SGS (Sub-Grid Scale) components, which are smaller than the computational grid cells. Large-scale eddies, i.e., the GS components of turbulence eddies, are directly numerically simulated without relying on the use of a physically simplified model. On the other hand, the main effect of small-scale eddies, i.e., the SGS components, is to dissipate energy, and this dissipation is modeled based on the physical considerations of the SGS stress.

For the governing equations of the flow, a spatially-filtered continuity equation for incompressible fluid (Eq. (1)) and a spatially filtered Navier-Stokes equation (Eq. (2)) are used:

$$\frac{\partial \bar{u}_i}{\partial x_i} = 0 \qquad \text{-(1)}$$

$$\frac{\partial \bar{u}_i}{\partial t} + \bar{u}_j \frac{\partial \bar{u}_i}{\partial x_j} = -\frac{\partial \bar{p}}{\partial x_i} + \frac{1}{\mathrm{Re}} \frac{\partial^2 \bar{u}_i}{\partial x_j \partial x_j} - \frac{\partial \tau_{ij}}{\partial x_j} \qquad \text{-(2)}$$

Supporting equations are given in Eqs. (3) - (8):

$$\tau_{ij} \approx \overline{u_i' u_j'} \approx \frac{1}{3}\overline{u_k' u_k'}\delta_{ij} - 2\nu_{SGS}\bar{S}_{ij} \qquad \text{-(3)}$$

$$\nu_{SGS} = \left(C_s f_s \Delta\right)^2 \left|\bar{S}\right| \qquad \text{-(4)}$$

$$\left|\bar{S}\right| = \left(2\bar{S}_{ij}\bar{S}_{ij}\right)^{1/2} \qquad \text{-(5)}$$

$$\bar{S}_{ij} = \frac{1}{2}\left(\frac{\partial \bar{u}_i}{\partial x_j} + \frac{\partial \bar{u}_j}{\partial x_i}\right) \qquad \text{-(6)}$$

$$f_s = 1 - \exp\left(-z^+ / 25\right) \qquad -(7)$$

$$\Delta = \left(h_x h_y h_z\right)^{1/3} \qquad -(8)$$

Because mean wind speeds of approximately 5 m/s or higher are considered in the present study, the effect of vertical thermal stratification (density stratification), which is generally present in the atmosphere, is neglected.

The computational algorithm and the time marching method are based on a FS (Fractional-Step) method[2] and the Euler explicit method, respectively. The Poisson's equation for pressure is solved by the SOR (Successive Over-Relaxation) method. For discretization of all the spatial terms in Eq. (2) except for the convective term, a second-order central difference scheme is applied. For the convective term, a third-order upwind difference scheme is applied. An interpolation technique based on four-point differencing and four-point interpolation by Kajishima[3] is used for the fourth-order central differencing that appears in the discretized form of the convective term. For the weighting of the numerical diffusion term in the convective term discretized by third-order upwind differencing, α = 3 is commonly applied in the Kawamura-Kuwahara Scheme[4]. However, α = 0.5 is used in the present study to minimize the influence of numerical diffusion. For LES subgrid-scale modeling, the commonly used Smagorinsky model[5] is adopted. A wall-damping function is used with a model coefficient of 0.1.

3. Terrain Elevation Data and Simulation Set-up

In this section, the terrain elevation data and simulation set-up are described. Fig. 2 shows a contour map created from the terrain elevation data adopted in the present study. As indicated in this figure, DEM data with a spatial resolution of 1 m were created using and based on the terrain data provided by Risø DTU as the original data. The wind direction considered in the simulation is 239°, where the wind direction is defined such that 0° indicates northerly wind.

Fig. 3 shows the evaluation points for the vertical profiles of airflow properties. In the present study, at four points (M1, M2, M3, and M4) on Line A which are defined for the study site of the Bolund Experiment, profiles of the mean wind velocity obtained from RIAM-COMPACT® and the wind tunnel experiment are compared. As shown in the figure, the mean wind velocity profile acquired for point M0 on Line A from the wind tunnel experiment is given at the inflow boundary in the numerical simulation.

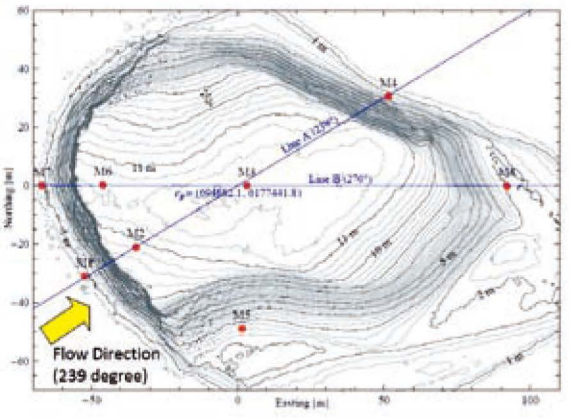

Fig. 2 Terrain elevation data used in the present study

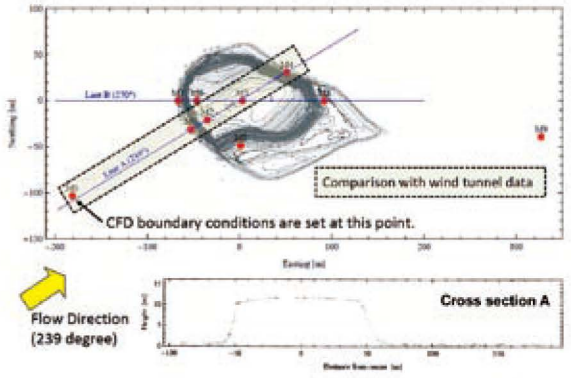

Fig. 3 Evaluation points for the vertical profiles of airflow properties.

Fig. 4 illustrates the computational domain, the computational grid, and the coordinate system used in the present study. The dimensions of the computational domain are 38.55H, 38.55H, and 15.45H for the streamwise (x), spanwise (y), and vertical (z) directions, respectively, where H (=11m) is the maximum terrain elevation within the computational domain. The vertical dimension of the computational domain is set identical to that of the wind tunnel in order to avoid blockage effect. The numbers of computational grid points in the x-, y-, and z-directions are set to 213, 213, and 65, respectively, which results in a total of approximately three million grid points. As for the spatial resolution, the grid points are spaced at an even interval of $\Delta x = \Delta y$ = 2m (= 0.18H) in the x-y cross section; the grid points are spaced at uneven intervals of Δz = 0.038m to

7.64m (0.003H to 0.7H) in the z-direction so that the grid cells are distributed with higher density in the vicinity of the ground surface. For the inflow conditions, as previously described in the discussion of Fig. 3, the mean wind velocity profile obtained at point M0 on Line A in the wind tunnel experiment is given at the inflow boundary. The characteristic wind velocity scale U_{ref} adopted in the present study is the value of the wind velocity at the inflow boundary at the height of the maximum terrain elevation, H (11m). The Reynolds number Re (= $U_{ref}H / \nu$), which is based on U_{ref} and H, is set to 2.8×10^4 in order to match the value from the wind tunnel experiment.

4. Overview of the Wind Tunnel Experiment

Subsequently, an overview of the wind tunnel experiment performed in the present study will be given. Fig. 5 shows a schematic view of the wind tunnel facility. This facility is the boundary layer wind tunnel of the Institute of Industrial Science, University of Tokyo. The dimensions of the test section are 16.5, 2.2 and 1.8m in length, width, and height, respectively. (See http://venus.iis.u-tokyo.ac.jp/equip/ for details.)

Measurements of the airflow field were made using a split-fiber probe, which is capable of detecting reversed flow (Fig. 6). The sampling intervals and the duration of the measurements were set to 1kHz and 60s, respectively.

Fig. 7 shows the terrain model created for the present study. The scale of the terrain model was 1/150, and the maximum terrain elevation H (11m) was approximately 7cm in the wind tunnel experiment (Fig. 7a). Fig. 7b is a close-up view of the terrain model. Fig. 8 shows a view of airflow measurements conducted in the wind tunnel (viewed from downstream). Spires and roughness blocks were placed upstream of the model, and a boundary layer flow, in which the vertical profile of the mean wind speed followed a 1/7 power law distribution, was generated.

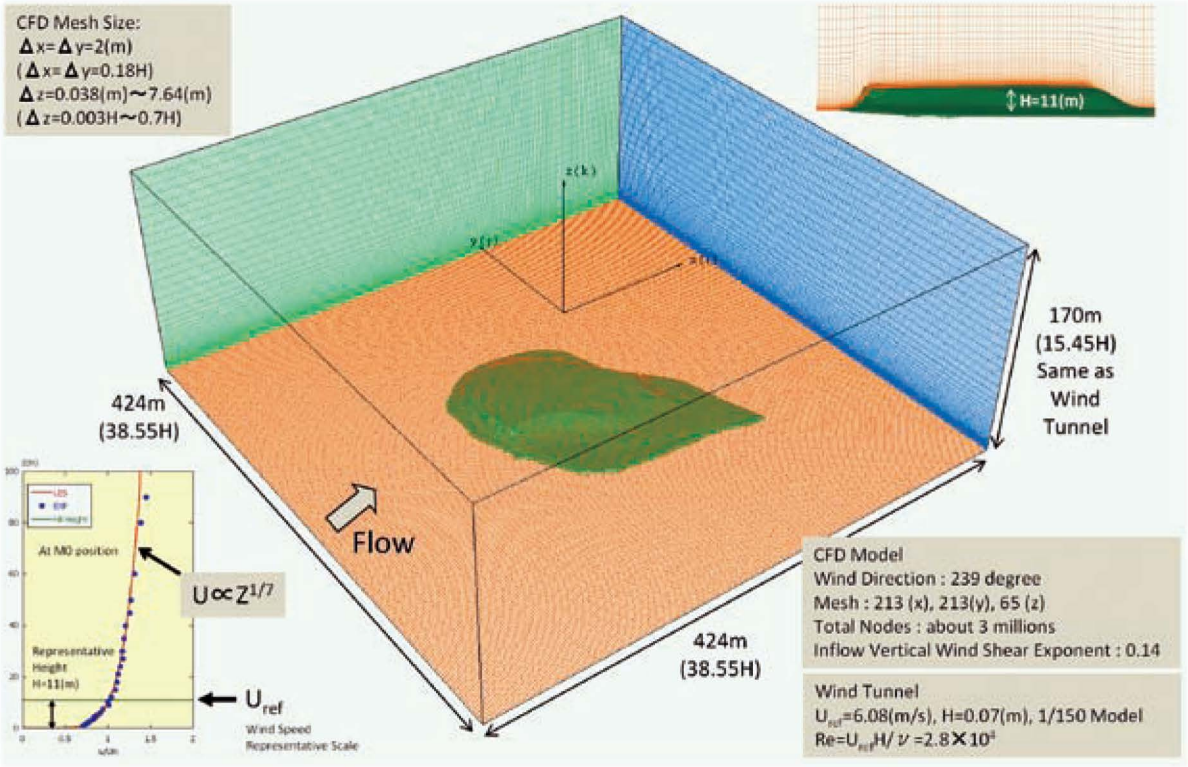

Fig. 4 Computational domain, computational grid, coordinate system, and other relevant information

風洞本体	測定部断面	2,200mm(幅)×1,800mm(高さ)
	測定胴長さ	161,470mm
	境界層長さ	12,850mm
	風速範囲	0.2～20m/s
送風機	型式	手動可変ピッチ付 低騒音型軸流送風機
	風量	80m³/sec
	静圧	80mmAq
電動機	型式	他力強制冷却型直流電動機
	容量	DC440V160kw
	回転数	0～1,150rpm
	制御	サイリスタ制御

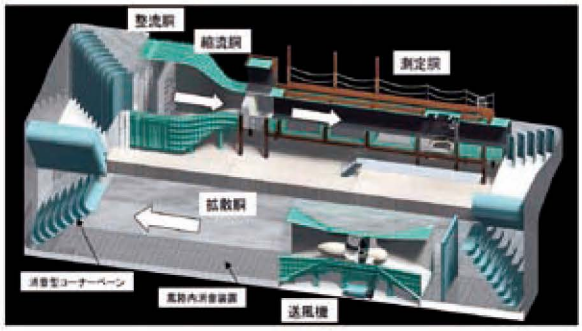

Fig. 5 The boundary layer wind tunnel used in the present study (test section length: 16.5 m, width: 2.2 m, height: 1.8 m), owned by the Institute of Industrial Science, University of Tokyo

Fig. 6 Split-fiber probe, capable of detecting reversed flow

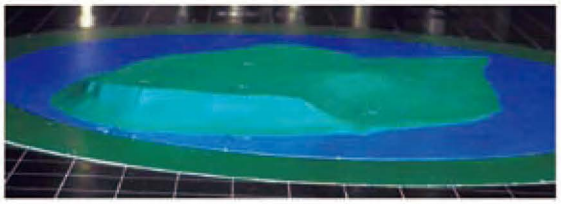

(a) Overall view

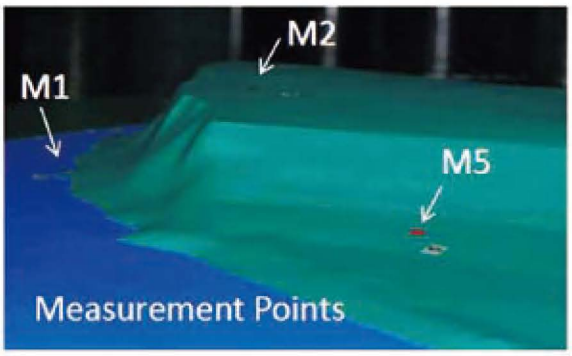

(b) Enlarged view

Fig. 7 Terrain model

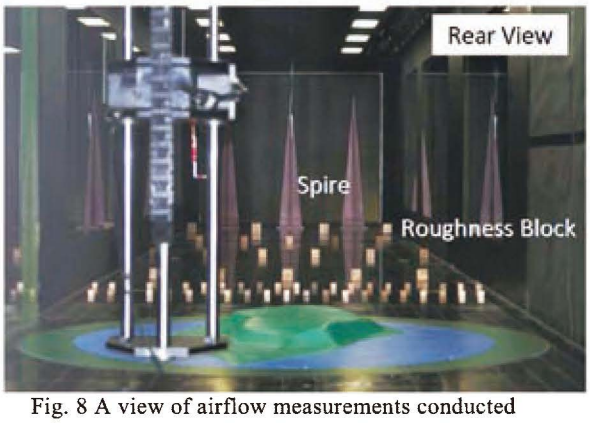

Fig. 8 A view of airflow measurements conducted in the wind tunnel, viewed from downstream

5. Results and Discussions

In this section, comparisons between the results from the numerical simulation (RIAM-COMPACT® LES turbulence model) and those from the wind tunnel experiment are discussed.

Fig. 9 shows visualization of the time-averaged (non-dimensional time: $t^* = 100 - 200$) wind fields obtained from the numerical simulation (RIAM-COMPACT® LES turbulence model). Specifically, the figure shows the distribution of the streamwise (x) velocity component. For comparison, the case in which the surface roughness was taken into consideration is also shown. The effect of the surface roughness was included by adding an external force term (a canopy model) to the governing equations as in Uchida and Ohya[6] (drag coefficient Cd = 10). This roughness model was applied to the air layer extending from the ground surface to $z^* \leqq 0.0286H$ (2mm in the wind tunnel), where H is the maximum terrain elevation (11m; 7cm in the wind-tunnel experiment), the characteristic length scale in the present study. This range for applying the roughness model was selected based on the results of the wind tunnel experiment. Examinations of the case with a smooth surface (Fig. 9a)

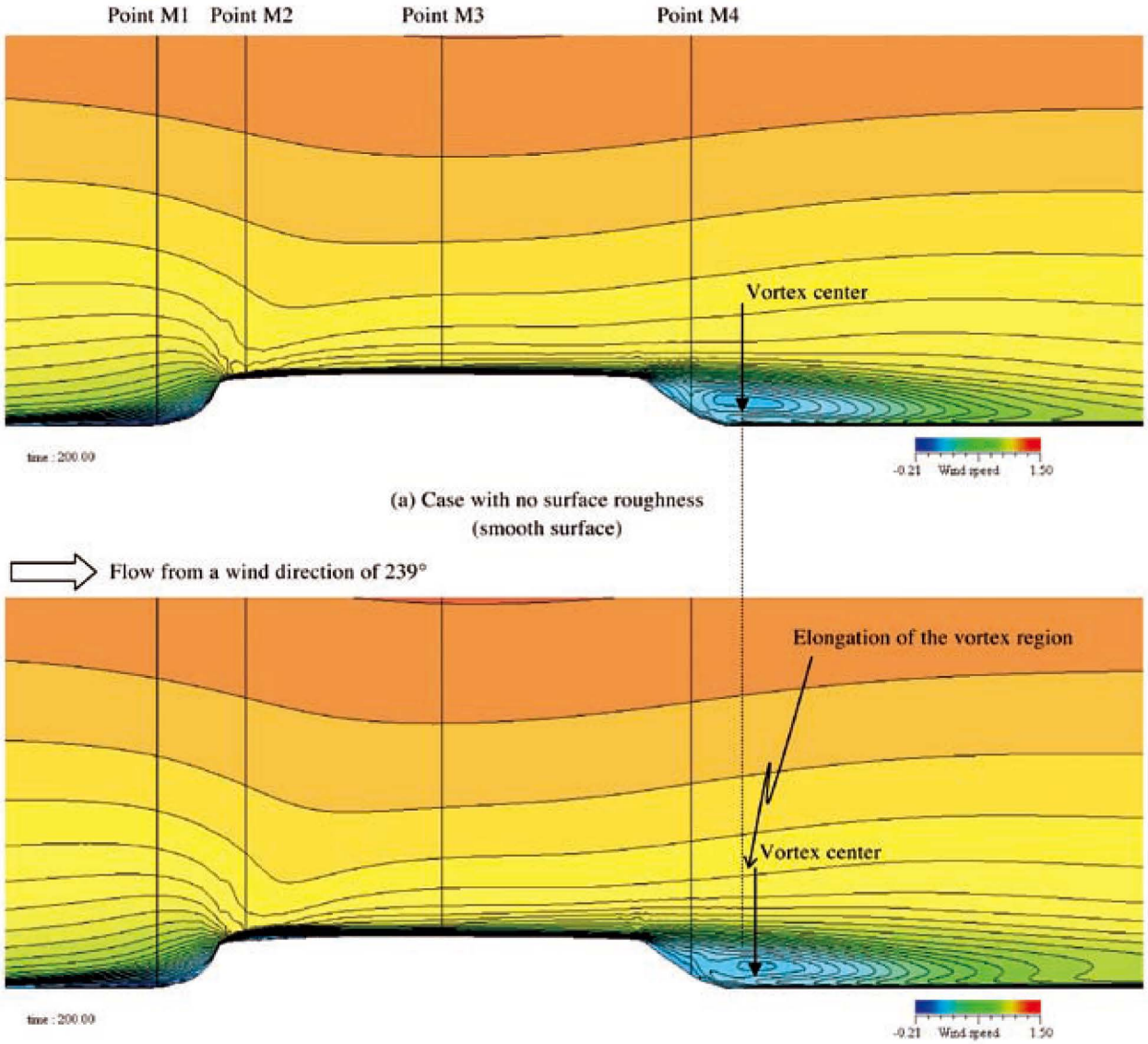

(b) Case with surface roughness
(rough surface)

Fig. 9 Results of the numerical simulations (RIAM-COMPACT® LES turbulence model).
Distribution of the time-averaged streamwise (x) velocity component (non-dimensional time: t^*= 100 - 200).

and the case with a rough surface (Fig. 9b) reveal that vortex regions are formed downstream of the hill. Fig. 9b clearly indicates elongation of the vortex region due to the effect of the surface roughness as noted in the figure[6].

In Fig. 10, the vertical profiles of the streamwise (x) wind velocity at points M1 to M4 indicated in Fig. 9 are compared. In this figure, lines, circles (○), and plus signs (+) indicate the results from the wind tunnel experiment (smooth surface), the LES numerical simulation (smooth surface), and the LES numerical simulation (rough surface), respectively. At all the examined points and heights, the results from the LES numerical simulations and wind tunnel experiment are in good agreement. Furthermore, at points M1 to M3, no significant differences due to the absence or presence of the surface roughness can be identified in the profiles of the mean wind velocity obtained from the LES numerical simulations. As described in the discussion of Fig. 9, the effect of the surface roughness is evident in

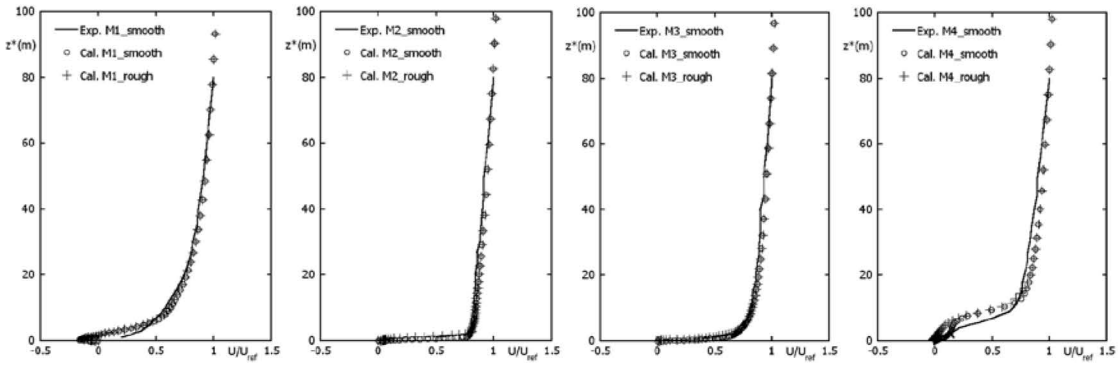

Fig. 10 Comparison between the numerical simulations (RIAM-COMPACT® LES turbulence model) and the wind tunnel experiment. Plotted for the four points M1 to M4 shown in Fig. 9.

Vertical profiles of the streamwise (x) wind velocity component.
- : wind tunnel experiment (smooth surface)
○ : LES numerical simulation (smooth surface), ＋: LES numerical simulation (rough surface)

the size of the vortex region formed downstream of the hill. As a result of this effect, in the vicinity of the ground surface at point M4, there exist differences in the values of the mean wind velocity in the vertical profiles between the case with a smooth surface and the case with a rough surface.

6. Summary

In the present study, wind conditions were numerically predicted for the site of the Bolund Experiment using the RIAM-COMPACT® natural terrain version software, which is based on an LES turbulence model (CFD). In addition, airflow measurements were made using a split-fiber probe in the boundary layer wind tunnel of the Institute of Industrial Science, University of Tokyo (a facility of the research group of Prof. Chisachi Kato). The characteristics of the airflow at and in the vicinity of the site of the Bolund Experiment were clarified. The study also examined the prediction accuracy of the LES turbulence simulations (CFD). The values of the streamwise (x) wind velocity predicted by the CFD model were generally in good agreement with those from the wind tunnel experiment at all points and heights examined, demonstrating the validity of CFD based on LES turbulence modeling.

Acknowledgements

The present study was partly funded by the New Energy and Industrial Development Organization (NEDO) "Research and Development for Wind Power and Other Natural Energy Technologies / Research and Development for Wind-power Generation Technologies of the Next Generation / Research and Development for Basic and Applied Technologies (Research and Development on International Standardization of Wind Turbine Performance Evaluation Techniques and Related Matters using Numerical Simulation Techniques), FY 2010 - 2012" and the Japan Society for the Promotion of Science (JSPS) "Grant-in-Aid for Scientific Research (B) (Grant Number 24310120), FY 2012 - 2014." I wish to express my gratitude to these funding agencies.

References

1) Uchida, T., Ohya, Y., Micro-siting Technique for Wind Turbine Generator by Using High Resolution Elevation Data, JSME International Journal 「Environmental Flows」, Series B, Vol.49, No.3 (2003), pp.567-575
2) Kim, J. and Moin, P., Application of a fractional-step method to incompressible Navier-Stokes equations, J. Comput. Phys., Vol.59 (1985), pp.308-323
3) Kajishima, T., Upstream-shifted interpolation method for numerical simulation of incompressible flows, Bull. Japan Soc. Mec. Eng. B, 60-578 (1994), pp.3319-3326, (in Japanese)
4) Kawamura, T., Takami, H. and Kuwahara, K., Computation of high Reynolds number flow around a circular cylinder with surface roughness, Fluid Dyn. Res., Vol.1 (1986), pp.145-162
5) Smagorinsky, J., General circulation experiments with the primitive equations, Part 1, Basic experiments, Mon. Weather Rev., Vol.91 (1963), pp.99-164

6) Uchida, T., Ohya, Y., Numerical. Study of Wind Characteristics around a Two-Dimensional. Escarpment in a Uniform Flow, Journal of Applied Mechanics, JSCE, Vol.8 (2005), pp.831-838 (in Japanese)